

Forgotten Right Ventricle in Pediatric Dilated Cardiomyopathy

Hala Mounir Agha¹ · Hossam Ibrahim¹ · Inas Abd El Satar¹ ·
Naglae Abd El Rahman¹ · Doaa Abd El Aziz¹ · Zeinab Salah¹ · Sonia El Saeidi¹ ·
Fatma Mostafa¹ · Wael Attia¹ · Mohamed Abd El Rahman¹ · Gaser Abd El Mohsen¹

Received: 31 July 2016 / Accepted: 10 February 2017 / Published online: 18 March 2017
© Springer Science+Business Media New York 2017

Abstract To evaluate the right ventricular (RV) function in relation to that of the left ventricle (LV) in patients with dilated cardiomyopathy (DCM). Echocardiographic examination was done using tissue Doppler imaging (TDI) and two-dimensional speckle tracking echocardiography (2D-STE) for 32 pediatric patients with DCM comparing them to another 32 normal matched controls. The global longitudinal strain (GLS) derived from 2D-STE was used to reflect the LV systolic function. Tricuspid annular plan systolic excursion (TAPSE) and the following RV TDI derived indexes: peak systolic velocity (S'), peak early diastolic velocity E' , peak late diastolic velocity A' , isovolumic acceleration (IVA) and myocardial performance index (MPI) were measured. RV had significant systolic and diastolic dysfunction; TAPSE, S' velocity, IVA, peak early diastolic velocity (E') and peak early diastolic velocity/peak late diastolic velocity (E'/A') ratio were significantly decreased while MPI was significantly prolonged compared to controls. Moreover, TAPSE, S' , IVA, E' , E'/A' and RV MPI were significantly correlated to LV GLS. For prediction of

LV dysfunction among patients, the area under the receiver operating characteristic curve was 0.98 for RV MPI, 0.906 for RV IVA. For identifying severe LV dysfunction; RV MPI >0.29 had 100% sensitivity and 93.7% specificity, while the RV IVA ≤ 3 had 84.4% sensitivity and 90.6% specificity. In pediatric patients with DCM the RV systolic and diastolic functions are affected beside the LV dysfunction. Non-conventional echocardiographic evaluation of RV function is recommended in among this cohort.

Keywords Dilated cardiomyopathy · Right ventricle · Tissue Doppler imaging · Isovolumic acceleration · 2D-speckle tracking

Abbreviations

2D-STE	2D speckle tracking echocardiography
ACEI	Angiotensin converting enzyme inhibitors
AUC	Area under curve
BSA	Body surface area

✉ Hala Mounir Agha
halaazza@gmail.com

Hossam Ibrahim
Hossam.Cardiology@gmail.com

Inas Abd El Satar
inassaad66@yahoo.com

Naglae Abd El Rahman
dnaglaa@hotmail.com

Doaa Abd El Aziz
doaa_abdulaziz@yahoo.com

Zeinab Salah
zeinabseliem@yahoo.com

Sonia El Saeidi
myheartclinic@windowslive.com

Fatma Mostafa
fatmaalzahraah@hotmail.com

Wael Attia
waelped@yahoo.com

Mohamed Abd El Rahman
moh-rahman1968@hotmail.com

Gaser Abd El Mohsen
gaser_abdelmohsen81@yahoo.com

¹ Pediatric Cardiology Division, Department of Pediatrics, Faculty of Medicine, Specialized Pediatric Hospital, Cairo University, Kasr Al Aini Street, Cairo 11562, Egypt

CUSPH	Cairo University Specialized Pediatric Hospital
DBP	Diastolic blood pressure
DCM	Dilated cardiomyopathy
DVD	Digital versatile disc
ECG	Electrocardiogram
EF	Ejection fraction
ET	Ejection time
FS	Fractional shortening
GE	General Electric
GLS	Global longitudinal strain
ICT	Isovolumic contraction time
IRT	Isovolumic relaxation time
IVA	Isovolumic acceleration
IVS	Interventricular septum
LA	Left atrium
LAD	Left atrial diameter
LV	Left ventricle
LVDD	Left ventricular diastolic diameter
LVLW	Left ventricular lateral wall
MAPSE	Mitral annular plan systolic excursion
MHz	Mega hertz
MPI	Myocardial performance index
MR	Mitral regurgitation
NT-pro-BNP	The N-terminal-pro brain natriuretic peptide
NYHA	New York Heart Association
PW	Pulsed wave
ROC	Receiver operating characteristic
RV	Right ventricle
SBP	Systolic blood pressure
SD	Standard deviation
SPSS	Statistical Package for Social Science
TAPSE	Tricuspid annular plan systolic excursion
TDI	Tissue Doppler imaging

Introduction

Dilated cardiomyopathy (DCM) is the most common form of cardiomyopathy in children; it is characterized by left ventricular (LV) dysfunction and dilatation with progressive heart failure that may lead to death. [1, 2]. In routine echocardiographic examination of these patients, most of the studies focus mainly on the assessment of the LV function forgetting the right ventricle (RV), because of its complex shape that prevents application of any geometrical assumption for its functional assessment. As the RV and the LV share the interventricular septum (IVS), their functions are closely linked together. The RV contains mainly transverse muscle fibers in its free wall in addition to sharing oblique fibers in the IVS with the LV, thus LV contraction contributes in the RV contraction via the IVS, that is why

assessment of RV function in these patients is of paramount importance [3]. Tissue Doppler imaging (TDI) is a modality that is present in most of available echocardiographic machines, it is used for assessment of the peak myocardial velocity and time, but this modality could be affected by the angle of ultrasound beams to the targeted myocardial wall in addition to being load dependent [4]. TDI could be also used for evaluation of isovolumic acceleration (IVA), the index of RV systolic function that may be load independent [5]. Two dimensional speckle tracking echocardiography (2D-STE) is a relative novel imaging modality providing an objective and quantitative evaluation of global and regional myocardial deformation independently from the ultrasound beam angle and cardiac translational movements, overcoming TDI limitations, yet it is limited by its low frame rates [6, 7].

The aim of this study was to evaluate the RV function in pediatric patients with idiopathic DCM using TDI, and to correlate it to the LV dysfunction evaluated by 2D-STE.

Patients and Methods

This is a prospective case–control study that was conducted on 32 pediatric patients who have been diagnosed as idiopathic DCM [8, 9]. Doppler velocities were measured for the mitral and tricuspid valves using apical four-chamber view; for the aortic valve using the apical five chamber view, and for the pulmonary valve using parasternal short-axis view. The following Doppler parameters were measured: mitral peak *E* and *A* wave velocities. LV Tei index was calculated from pulsed wave (PW) Doppler as the sum of isovolumic contraction time (ICT) and isovolumic relaxation time (IRT) divided by ventricular ejection time (ET) ($Tei = (ICT + IRT) / ET$) [10], where cursor line was placed midway between anterior mitral leaflet and LV outflow in the same cycle [11], while RV Tei index was measured using this formula $(a - b) / b$, where “a” is the time between the end of A wave of tricuspid inflow to the beginning of E wave of tricuspid inflow in the next cardiac cycle obtained by PW Doppler at tricuspid inflow at apical four chamber view, and “b” is the pulmonary ET obtained by PW Doppler at pulmonary valve in parasternal short axis view. To reduce the effect of respiration on blood velocities and as breath holding is not applicable in young children, three cardiac cycles were recorded and the average velocity was measured. Color Doppler was used for detection and grading of mitral regurgitation (MR) by tracing the vena contracta and the regurgitant jet area relative to the left atrium (LA) area, regurgitation was graded as mild, moderate and severe. **Tissue Doppler imaging (TDI)**: PW-TDI was done, care was taken to increase the frame rate to be more than 180 frames/s (by decreasing sector width

and depth) to improve temporal resolution; moreover care was taken also to align the ultrasound beam parallel to the target wall during measurements (interrogation angle not more than 15°). To reduce the effect of respiration on tissue velocities, three cardiac cycles were recorded and the average velocity and times were calculated. The following parameters were measured: systolic (S') and diastolic (E' , A' , E'/A' ratio) myocardial velocities at the basal segments of the LV lateral wall (LVLW), septal wall, and RV free wall. Myocardial performance index (MPI, Tei index): intervals measurements were performed within one cardiac cycle. The Tei index was calculated as: $Tei = (ICT + IRT) / ET$, for MPI of the RV PW-TDI tracing was applied at tricuspid annulus, for LV using PW-TDI tracing was applied at the lateral mitral annulus and basal septum [12, 13]. IVA at tricuspid annulus, basal septum, LVLW in apical four chamber view, $IVA = \text{peak } S_1 / \text{acceleration time of } S_1$ (time from the start of S_1 to the peak of S_1) [5]. **2D speckle tracking echocardiography (2D-STE)**: 2D-STE was done for LV only (although it can be done for the RV using the LV software but we thought that the different geometry of the RV makes this method questionable). 2D images were obtained in the apical four chambers, apical long axis and apical two chamber views for measurement of longitudinal deformation. Frame rates 60–90 Hz were used, because these rates are thought to be optimal for 2D-STE [14]. Data were stored; acceptable images from three cardiac cycles were digitally saved in cine loop format on the hard disc of the echo machine then exported to a digital versatile disc (DVD) then imported to a software installed on the computer [Echo PAC version 11, General Electric (GE)] for offline speckle-tracking analysis. Cardiac cycles with length more than 10% different from the mean length of

the three cardiac cycles were excluded from further analysis, manual tracking of the endocardial borders have been done. The timing of aortic valve closure was also manually determined. Care was taken to keep the heart rate in the same range in the stored loops. Tracking was accepted not only if the Echo PAC software showed adequate tracking, but also if the examiner’s inspection revealed good tracking throughout the cardiac cycle. Q analysis: 2D strain was used, global longitudinal strain (GLS) was measured using 18 segments Bull’s eye as shown in Fig. 1.

Statistical Analysis

Statistical analysis was performed using Statistical Package for Social Science (SPSS, Chicago, Illinois, USA, version 19). Data were tested for normality using Kolmogorov, Smirnov and Shapiro tests, normally distributed data were expressed as mean ± SD (standard deviation), non-normally distributed data were expressed as median and interquartile range (25th and 27th percentiles), and categorical data were summarized as percentages. Comparisons between groups were calculated using: nonparametric Mann–Whitney test for non-normally distributed data, Student’s T test for normally distributed data and χ^2 test for categorical data. Correlation between variables was evaluated using Pearson and Spearman correlation coefficients. Receiver-operating characteristic (ROC) curves for RV indexes were constructed for the prediction of severity of LV dysfunction among patients. The ROC curve was used to define the best cut-off point that gives the highest sensitivity and specificity. Graphs were done using MedCalc for Windows, version 15.0 (MedCalc Software, Ostend, Belgium). P -values <0.05 were considered significant.

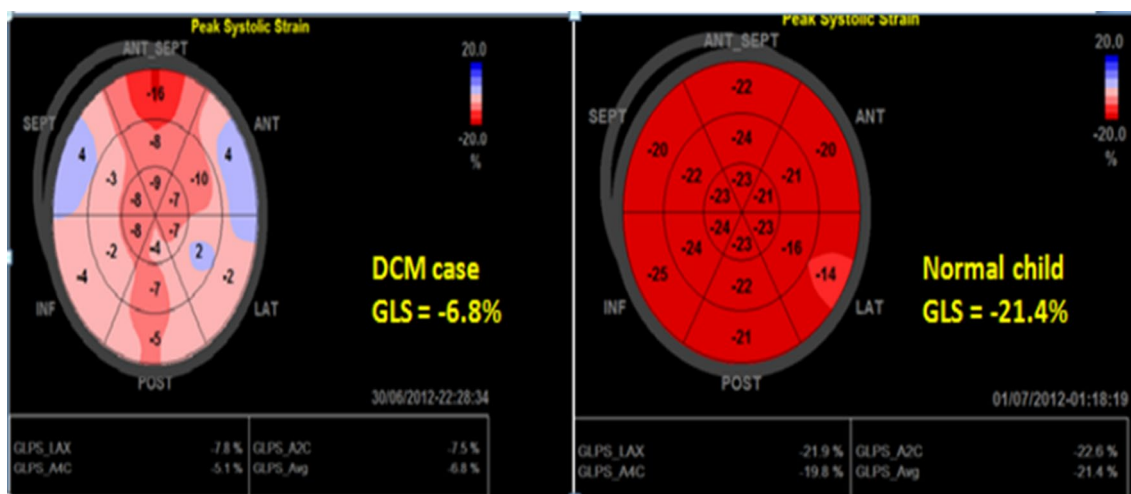


Fig. 1 Bull’s eye of global longitudinal strain of left ventricle in a patient with dilated cardiomyopathy (left) compared to a normal child (right). Note the markedly reduced GLS in this patient. *DCM* dilated cardiomyopathy, *GLS* global longitudinal strain

Table 1 Clinical data of the studied groups

	Patients (<i>n</i> =32)	Controls (<i>n</i> =32)	<i>P</i> values
Age (years) ^a	5 (2.3–8)	5.88 ± 3.92	0.67
Weight (kg) ^a	16.1 (10.88–22.98)	17.25 (14–20.75)	0.24
Height (cm) ^β	106.83 ± 20.92	116.32 ± 21.096	0.11
BSA (m ²) ^β	0.71 ± 0.24	0.79 ± 0.293	0.24
Heart rate ^β	103 ± 20	110 ± 18	0.74
SBP (mmHg) ^β	98 ± 15.12	94.2 ± 12.3	0.23
DBP (mmHg) ^β	58.50 ± 13.27	59 ± 11.8	0.35
Sex			
Male <i>n</i> (%)	19 (59.4%)	20 (62.5%)	0.79
Female <i>n</i> (%)	13 (40.6%)	12 (37.5%)	

Clinical data of the studied groups, as noted: the patient group and control were matched (*P* > 0.05),

BSA body surface area, SBP systolic blood pressure, DBP diastolic blood pressure

^aData are expressed as median and interquartile range (25th–75th percentile)

^βData are expressed as mean ± SD

Table 2 Right ventricular parameters of the studied groups

	Patients (<i>n</i> =35)	Controls (<i>n</i> =32)	<i>P</i> values
TAPSE (mm) ^b	17 (15–19.75)	20.5 (18.25–23)	0.0001
<i>S'</i> RV (cm/s) ^b	10 (8–13)	14 (13–17.5)	<0.0001
IVA RV (m/s ²) ^b	2 (1.5–3)	4.3 (3.8–5.2)	<0.0001
<i>E'</i> velocity RV (cm/s) ^a	11.59 ± 4.30	17.62 ± 3.09	<0.0001
<i>A'</i> velocity RV (cm/s) ^a	10.06 ± 3.36	11.00 ± 2.46	0.208
<i>E'/A'</i> ratio LW RV ^a	1.27 ± 0.59	1.65 ± 0.36	<0.01
RV MPI by Doppler ^b	0.42 (0.30–0.60)	0.10 (0.06–0.18)	<0.0001
RV MPI by TDI ^b	0.50 (0.43–0.60)	0.25 (0.22–0.27)	<0.0001

Right ventricular parameters of the studied groups, as noted: there is significant RV systolic and diastolic dysfunction in patients compared to control, as the RV systolic parameters (TAPSE, *S'*, IVA) and diastolic parameters (*E'*, *E'/A'* ratio) are markedly reduced while MPI is markedly prolonged in patient group

TAPSE tricuspid annular plan systolic excursion, IVA isovolumic acceleration, LW lateral wall, RV right ventricle, MPI myocardial performance index, TDI tissue Doppler imaging

^aData are expressed as mean ± SD

^bData are expressed as median and interquartile range (25th, 75th percentile)

Results

Demographic and clinical characteristics of the studied population were shown in Table 1. 90% of patients were New York Heart Association (NYHA) II and III, and 65.6% had MR grade II.

RV Function

The RV of our cohorts showed significant systolic and diastolic dysfunction compared to the controls as tricuspid annular plan systolic excursion (TAPSE), *S'*, IVA, *E'* and *E'/A'* ratio were significantly reduced in the patient group, on the other hand, Doppler derived MPI and TDI derived MPI were significantly prolonged compared to the controls (Table 2; Figs. 2, 3, 4). Moreover RV indexes; TAPSE, *S'*, IVA, *E'*, *E'/A'* and MPI by TDI were correlated to GLS of LV while TAPSE was negatively correlated to the degree of MR (Table 4).

LV Function

The LV of the studied patients had systolic impairment compared to the controls. The GLS was reduced in patients. Like GLS, the FS, ejection fraction (EF), MAPSE, *S'* at basal septum, *S'* at LVLW, IVA at the septum, IVA at LVLW all showed significant reduction (*P* < 0.0001). The diastolic function of LV was also impaired in cases compared to controls, as *E'* at the septum, *E'* at LVLW, showed significant decrease in cases (*P* < 0.0001), but the mitral *E'/average E'* (at the septum and LVLW) was significantly higher in patients denoting elevated LV diastolic pressure and left atrial pressure and hence LV diastolic impairment. The MPI of patients showed significant prolongation in comparison to the control group for both Doppler derived MPI and TDI derived MPI (Table 3). The GLS was significantly correlated to LV systolic and diastolic parameters (Table 4).

ROC Curve Analysis

For prediction of severe LV dysfunction among patients, the area under the ROC curve was 0.98 for RV MPI, 0.906 for RV IVA. For identifying severe LV dysfunction; RV MPI > 0.29 had 100% sensitivity and 93.7% specificity, while the RV IVA ≤ 3 had 84.4% sensitivity and 90.6% specificity (Table 5; Fig. 5).

Discussion

The RV is usually forgotten during echocardiographic assessment of DCM patients. This is due to its complex shape that does not fit with any geometrical assumption, subsequently the majority of the studies was focusing on LV assessment. In the present study, we studied the right as well as the LV systolic and diastolic functions

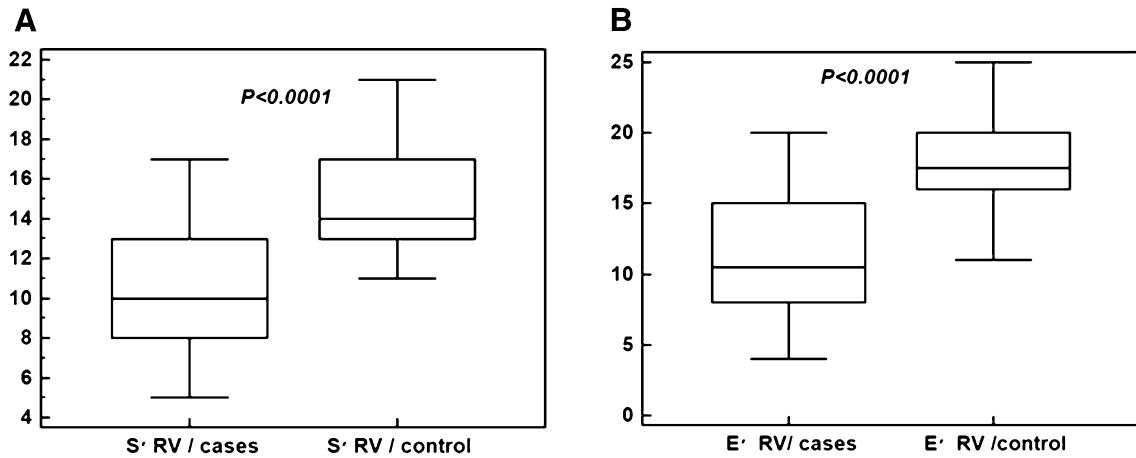


Fig. 2 Box (whisker) plot for RV systolic velocity (*S'*, left) and RV early diastolic velocity (*E'*, right) in patients and control groups. The RV *S'* and RV *E'* are markedly reduced in patients compared to control. *RV* right ventricle

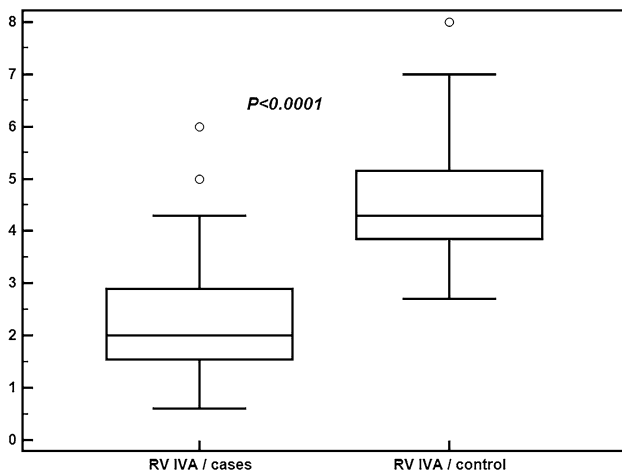


Fig. 3 Box (whisker) plot for RV IVA in patients and control groups. Note the markedly reduced RV IVA in cases compared to control. *RV IVA* right ventricular isovolumic acceleration

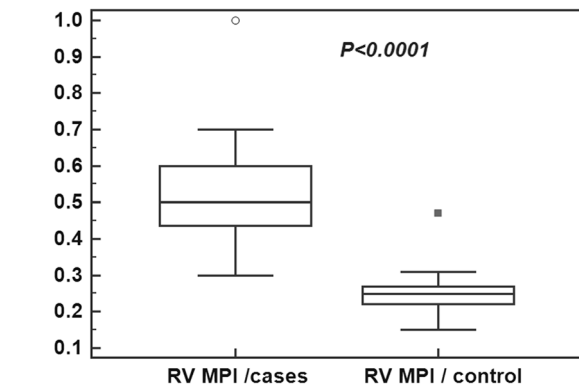


Fig. 4 Box (whisker) plot for TDI derived RV MPI in patients and control groups. Note the marked prolongation of RV MPI in cases compared to control. *TDI* tissue Doppler imaging, *RV* right ventricle, *MPI* myocardial performance index

combining TDI and 2D-STE together with the conventional echocardiographic parameters.

RV dysfunction among patients was evident in the present study; we assume that RV dysfunction among this cohort is related to ventricular interaction or secondary to the disease itself that may affect both ventricles but in a different patterns.

Patient Characteristics

The DCM patients and controls were matching regarding age, sex, weight and body surface area (BSA) (Table 1). The heart rate didn't show significant change between the two groups despite >90% of the patients were NYHA II and III and 65.6% of them had MR grade II. This finding

might be due the effect of digoxin and carvedilol treatment on the heart rate.

Right Ventricular Function of the Studied Groups

The RV of our cohort had significant systolic dysfunction compared to controls, as TAPSE, *S'* and IVA were reduced (Table 2), RV indexes among patients were significantly correlated to the LV GLS, this might be due the close link between LV and RV functions among this cohort. The RV has mainly transverse muscle fibers in its free wall in addition to sharing oblique fibers in the IVS with the LV, subsequently its contraction augments RV contraction; a condition defined as systolic ventricular interaction. The impaired LV systolic and diastolic functions in DCM together with MR lead to pulmonary venous congestion and pulmonary hypertension increasing the RV after load,

Table 3 Left ventricular parameters of the studied groups

Parameters	Patients (<i>n</i> = 32)	Controls (<i>n</i> = 32)	<i>P</i> values
M-mode parameters			
FS (%) ^a	20 (16 to 23)	37 (35 to 42)	<0.0001
EF (%) ^a	40 (33 to 45)	68 (65 to 74)	<0.0001
LA diameter (cm) ^a	2.9 (2.62 to 3.35)	2.2 (2 to 2.40)	<0.0001
LVDD (cm) ^b	5 ± 0.68	3.49 ± 0.61	<0.0001
MAPSE septum (mm) ^a	6 (5 to 8)	11 (10 to 12)	<0.0001
MAPSE LVLW (mm) ^a	7 (5 to 9)	11 (10 to 13)	<0.0001
STE/TDI systolic parameters			
GLS ^a	−11.5 (−7.12 to −14.38)	−22.8 (−20.42 to −24.68)	<0.0001
<i>S'</i> septum (cm/s) ^a	4.5 (4 to 5)	8 (7 to 9)	<0.0001
<i>S'</i> LVLW (cm/s) ^a	4 (3 to 5.75)	9 (8 to 10)	<0.0001
IVA septum (m/s ²) ^a	1.1 (0.9 to 1.4)	3.2 (2.5 to 3.8)	<0.0001
IVA LVLW (m/s ²) ^a	0.8 (0.6 to 1.4)	2.6 (1.9 to 3.2)	<0.0001
Diastolic parameters			
<i>E</i> mitral (cm/s) ^b	88.2 ± 28.70	100.8 ± 12.84	0.001
<i>A</i> mitral (cm/s) ^b	49.47 ± 18.52	57.78 ± 10.25	<0.05
<i>E/A</i> mitral ^a	1.87 (1.35 to 2.42)	1.8 (1.6 to 1.94)	0.314
<i>E'</i> septal (cm/s) ^b	6.97 ± 2.33	13.60 ± 2.46	<0.0001
<i>A'</i> septal (cm/s) ^a	4 (4 to 5.75)	7 (6 to 8)	<0.0001
<i>E'/A'</i> septal ^b	1.60 ± 0.70	2 ± 0.56	<0.05
<i>E'</i> LW (cm/s) ^a	7 (4.25 to 10)	16 (15 to 18)	<0.0001
<i>A'</i> LW (cm/s) ^a	4 (3 to 5)	7 (6 to 8)	<0.0001
<i>E'/A'</i> lateral ^a	1.67 (1 to 2.62)	2.33 (1.8 to 2.67)	<0.05
Average <i>E'</i> (cm/s) ^a	7 (5.12 to 8.88)	14.75 (13.12 to 16.5)	<0.0001
Mitral <i>E/average E'</i> ^a	12.95 (8.46 to 17.28)	6.61 (6.14 to 7.64)	<0.0001
Tei index			
MPI by Doppler ^a	0.60 (0.50 to 0.80)	0.20 (0.12 to 0.28)	<0.0001
MPI by TDI ^a	0.64 (0.60 to 0.80)	0.31 (0.27 to 0.35)	<0.0001

Left ventricular parameters of the studied groups, as shown the LV of patients has significant systolic and diastolic dysfunction, as MAPSE, EF, FS, GLS, IVA, *S'*, *E'*, *E'/A'* ratio are significantly decreased while MPI is significantly increased in patients compared to control

GLS global longitudinal strain, FS fractional shortening, EF ejection fraction, LVDD left ventricular diastolic diameter, LAD left atrial dimension, MAPSE mitral annular plane systolic excursion, IVA isovolumic acceleration, LV left ventricle, LW lateral wall, MPI myocardial performance index, TDI tissue Doppler imaging

^aData are expressed as median and interquartile range (25th, 75th percentile)

^bData are expressed as mean ± SD

thus making RV contraction more dependent on the oblique septal fibers which are mechanically more efficient than the free wall transverse fibers. As the global LV deformation is markedly diminished (including the IVS containing these oblique fibers) this leads to decreased systolic ventricular interaction, and reduction of RV deformation. Moreover, as the LV acquires more spherical shape, the septal fibers become less oblique decreasing their mechanical efficiency with more and more deterioration of RV deformation [3].

The RV diastolic function in our cohort was also impaired compared to controls, also RV *E'* velocity and RV *E'/A'* ratio were significantly correlated to LV GLS confirming the interrelation between both ventricles. These

findings could be interpreted as the IVS is in common share, RV systolic dysfunction leads to increase in RV diastolic pressure and LV dilatation might compress the RV cavity reducing the filling of RV and hence adding to the elevation of end diastolic pressure and diastolic dysfunction [3, 15, 16].

The RV MPI either measured by TDI or conventional Doppler was significantly prolonged in cases compared to controls. Previous publications reported similar findings [3, 16]. Interestingly, the TDI derived RV MPI could discriminate between patients and normal individuals with a very high sensitivity (100%) and specificity (93.6%) with a cut-off value >0.29, with significant correlation to LV GLS,

Table 4 Correlation between LV and RV parameters

Correlated parameters	Correlation coefficients	P values
GLS		
RV systolic parameters		
TAPSE	-0.675	<0.0001
IVA RV	-0.337	0.05
S' RV	-0.631	<0.0001
RV diastolic parameters		
RV E'	-0.572	0.001
RV E'/A'	-0.378	<0.05
RV MPI by TDI	0.438	0.01
LV systolic parameters		
LVLW S'	-0.701	<0.0001
FS	-0.657	<0.0001
MAPSE	-0.796	<0.0001
LV diastolic parameters		
LVLW E	-0.578	<0.0001
LV E septum	-0.657	<0.0001
LV MPI at LW by TDI	0.533	<0.01
TAPSE		
MR degree	-0.397	<0.05

Correlation between LV and RV parameters, as shown: the GLS of LV has significant correlation with RV systolic and diastolic parameters denoting the ventricular interaction, also GLS is significantly correlated to LV systolic and diastolic parameters

GLS global longitudinal strain, FS fractional shortening, TAPSE tricuspid annular plane systolic excursion, RV right ventricle, MAPSE mitral annular plane systolic excursion, MR mitral regurgitation, LV left ventricle, LW lateral wall, TDI tissue Doppler imaging. MPI myocardial performance index, IVA isovolumeic acceleration

so this index might be used on routine echocardiographic evaluation in such patients.

Most of the RV parameters like TAPSE, S', E', A' velocities are load dependent varying with respiration and different loading conditions, unlike IVA which is load independent. IVA in our cohort was significantly correlated to LV

GLS with a high sensitivity (84.4%) and specificity (90.6%) for prediction of LV dysfunction, hence it is useful in RV systolic function assessment.

LV Dysfunction

As previous published data, the LV of our cohort were significantly dilated with impaired systolic function as assessed by conventional parameters like FS, EF and MAPSE. These parameters represent the longitudinal shortening of LV and easy sensitive tools of LV systolic function [17–19]. Moreover FS and MAPSE were significantly correlated to LV GLS assessed by 2D-STE.

TDI LV S' velocity at both septum and lateral walls as well as IVA were significantly reduced in patients and correlated to LV GLS [15, 20]. 2D-STE derived LV GLS can evaluate the regional and global myocardial deformation overcoming the limitations of the conventional methods and TDI derived velocities and strain. In our cohort, LV GLS were significantly reduced with very high sensitivity and specificity and significantly correlated to LV systolic parameters measured by conventional methods and TDI, similarly to published data [2, 21].

Our studied patients had significant diastolic dysfunction with elevated LV diastolic pressure compared to controls, moreover the GLS was correlated to E' velocity at the septum and LVLW. This finding might be explained by systolic contribution to diastolic function through diastolic recoil of the myocardium from tension stored in systole. During systole, the myocardium twists and shortens, during diastole, rapid lengthening and untwisting creating suction force enhancing early filling, so diastole is dependent on the systole. Moreover systole is dependent on diastole and ventricular filling through the Frank–Starling mechanism. Therefore, assessment of the relation between systolic and diastolic dysfunction may be of paramount importance than evaluation of each function in isolation [22–25].

Table 5 ROC curve analysis of RV and LV parameters

	Sensitivity (%)	Specificity (%)	Cut-off values	AUC (95% confidence interval)	P values
TAPSE	62.5	87.5	≤17	0.74 (0.62–0.84)	<0.001
S' RV	71.9	90.6	≤12	0.87 (0.76–0.94)	<0.0001
IVA RV	84.4	90.6	≤3	0.91 (0.82–0.97)	<0.0001
E' RV	71.9	87.5	≤14	0.86 (0.75–0.93)	<0.001
MPI(TDI)	100	93.7	>0.29	0.98 (91.6–0.99)	<0.0001
GLS	96.9	100	>-18.1	0.99 (94–1.00)	<0.0001

ROC curve analysis of RV and LV parameters showing the higher sensitivity and specificity of RV IVA, RV MPI, and LV GLS for prediction of LV dysfunction

ROC receiver operating characteristic, TAPSE tricuspid annular plane systolic excursion, RV right ventricle, LV left ventricle, IVA isovolumic acceleration, MPI myocardial performance index, TDI tissue Doppler imaging, AUC area under the curve, GLS global longitudinal strain

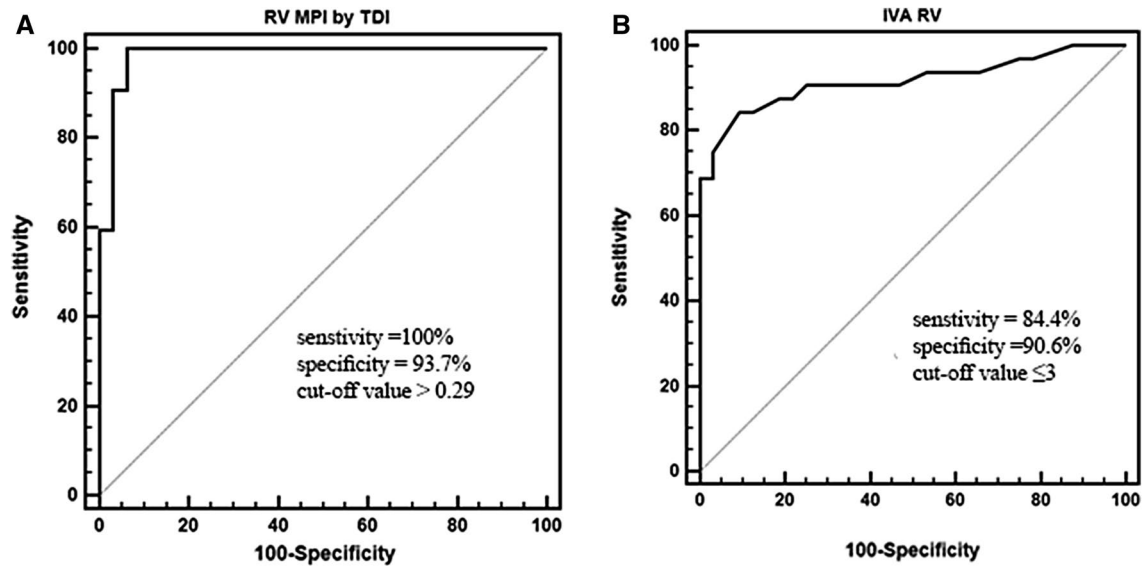


Fig. 5 ROC curve for TDI derived RV MPI (a) and RV IVA (b), showing high sensitivity and specificity of these parameters for prediction of LV dysfunction in pediatric dilated cardiomyopathy. ROC

receiver operating characteristic, *TDI* tissue Doppler imaging, *RV* right ventricle, *IVA* isovolumic acceleration, *MPI* myocardial performance index

Conclusion

In pediatric DCM patients, RV had significant systolic and diastolic dysfunction mainly elicited by TDI beside LV affection secondary to the interventricular interaction. TDI and 2D-STE add value on interpreting the findings and the dependency of LV systolic and diastolic functions on each other in DCM patients in children. RV assessment using TDI and LV evaluation using TDI and 2D-STE should be part of routine echocardiographic examination in pediatric DCM patients.

Study limitations

The main limitations of the study were; (1) all patients were on anti-failure measures, so we couldn't test the effect of treatment on cardiac function, (2) most of our studied cases had not tricuspid regurgitation or the regurgitation jet had poor signal, so evaluation of pulmonary arterial pressure was difficult, and (3) the N-terminal-pro brain natriuretic peptide (NT-pro-BNP) wasn't assessed and might be of value to correlate with the echocardiographic findings.

Acknowledgements The authors thank the Science and Technology Development Fund in Egypt (STDF) for the technical support during the period of research.

Compliance with Ethical Standards

Conflict of interest There are no conflicts of interest to declare.

References

1. Park MK (2008) Park's pediatric cardiology for practitioners, 5th edn. Mosby, St. Louis, p 261
2. Luk A, Ahn E, Soor GS, Butany J (2009) Dilated cardiomyopathy: a review. *J Clin Pathol* 62:219–225
3. Schwarz K, Singh S, Dawson D, Frenneaux MP (2013) Right ventricular function in left ventricular disease: pathophysiology and implications. *Heart Lung Circ* 22:507–511
4. Kukulski T, Hübbert L, Arnold M, Wranne B, Halte L, Sutherland GR (2000) Normal regional right ventricular function and its change with age: a Doppler myocardial imaging study. *J Am Soc Echocardiogr* 13:194–204
5. Vogel M, Schmidt M, Kristiansen S, Cheung M, White P, Sorensen K, Redington A (2002) Validation of myocardial acceleration during isovolumic contraction as a novel noninvasive index of right ventricular contractility: comparison with ventricular pressure–volume relations in an animal model. *Circulation* 105:1693–1699
6. Blessberger H, Binder T (2010) Non-invasive imaging: two dimensional speckle tracking echocardiography: basic principles. *Heart* 96:716–722
7. Geyer H, Caracciolo G, Abe H, Wilansky S, Carerj S, Gentile F, Nesser HJ, Khandheria B, Narula J, Sengupta PP (2010) Assessment of myocardial mechanics using speckle tracking echocardiography: fundamentals and clinical applications. *J Am Soc Echocardiogr* 23:351–369
8. Ghio S, Recusani F, Klersy C, Sebastiani R, Laudisa ML, Campana C, Gavazzi A, Tavazzi L (2000) Prognostic usefulness of the tricuspid annular plane systolic excursion in patients with congestive heart failure secondary to idiopathic or ischemic dilated cardiomyopathy. *Am J Cardiol* 85:837–842
9. López-Candales A, Rajagopalan N, Gulyasy B, Edelman K, Bazaz R (2007) Comparative echocardiographic analysis of mitral and tricuspid annular motion: differences explained with proposed anatomic-structural correlates. *Echocardiography* 24:353–359

10. Tei C, Dujardin KS, Hodge DO, Bailey KR, McGoon MD, Tajik AJ, Seward SB (1996) Doppler echocardiographic index for assessment of global right ventricular function. *J Am Soc Echocardiogr* 9:838–847
11. Quiñones MA, Otto CM, Stoddard M, Waggoner A, Zoghbi WA (2002) Recommendations for quantification of Doppler echocardiography: a report from the Doppler Quantification Task Force of the Nomenclature and Standards Committee of the American Society of Echocardiography. *J Am Soc Echocardiogr* 15:167–184
12. Rojo EC, Rodrigo JL, Pérez de Isla L, Almeria C, Gonzalo N, Aubele A, Cinza R, Zamorano J, Macaya C (2006) Disagreement between tissue Doppler imaging and conventional pulsed wave Doppler in the measurement of myocardial performance index. *Eur J Echocardiogr* 7:356–364
13. Ayhan SS, Özdemir K, Kayrak M, Bacaksiz A, Vatankulu MA, Eren Ö, Koc F, Duman C, Gülec H, Demir K, Ari H, Sönmez O, Gök H (2012) The evaluation of doxorubicin-induced cardiotoxicity: comparison of Doppler and tissue Doppler-derived myocardial performance index. *Cardiol J* 19:363–368
14. Teske AJ, De Boeck BWL, Melman PG, Sieswerda GT, Doevendans PA, Cramer MJ (2007) Echocardiographic quantification of myocardial function using tissue deformation imaging, a guide to image acquisition and analysis using tissue Doppler and speckle tracking. *Cardiovasc Ultrasound* 5:27
15. McMahan CJ, Nagueh SF, Eapen RS, Dreyer WJ, Finkelshtyn I, Cao X, Eidem BW, Bezold LI, Denfield SW, Towbin JA, Pignatelli RH (2004) Echocardiographic predictors of adverse clinical events in children with dilated cardiomyopathy: a prospective clinical study. *Heart* 90:908–915
16. Groner A, Yau J, Lytrivi ID, Ko HH, Neilsen JC, Parness IA, Srivastava S (2013) The role of right ventricular function in paediatric idiopathic dilated cardiomyopathy. *Cardiol Young* 23:409–415
17. Bergenzaun L, Öhlin H, Gudmundsson P, Willenheimer R, Chew MS (2013) Mitral annular plane systolic excursion (MAPSE) in shock: a valuable echocardiographic parameter in intensive care patients. *Cardiovasc Ultrasound* 11:16
18. Koestenberger M, Nagel B, Ravekes W, Avian A, Heinzl B, Fritsch P, Fandl A, Rehak T, Gamillscheg A (2012) Left ventricular long-axis function: reference values of the mitral annular plane systolic excursion in 558 healthy children and calculation of z-score values. *Am Heart J* 164:125–131
19. Taşolar H, Mete T, Çetin M, Altun B, Balli M, Bayramoğlu A, Otlu YÖ (2015) Mitral annular plane systolic excursion in the assessment of left ventricular diastolic dysfunction in obese adults. *Anatol J Cardiol* 15(7):558–564
20. Mohammed A, Friedberg MK (2008) Feasibility of a new tissue Doppler based method for comprehensive evaluation of left-ventricular intra-ventricular mechanical dyssynchrony in children with dilated cardiomyopathy. *J Am Soc Echocardiogr* 21:1062–1067
21. Meluzin J, Spinarova L, Hude P, Krejci J, Poloczkova H, Podrouzkova H, Pesl M, Orban M, Dusek L, Korinek J (2009) Left ventricular mechanics in idiopathic dilated cardiomyopathy: systolic–diastolic coupling and torsion. *J Am Soc Echocardiogr* 22:486–493
22. Firstenberg MS, Smedira NG, Greenberg NL, Prior DL, McCarthy PM, Garcia MJ, Thomas JD (2001). Relationship between early diastolic intraventricular pressure gradients, an index of elastic recoil, and improvements in systolic and diastolic function. *Circulation* 104:I330–I335
23. Granzier HL (2004) The giant protein titin: a major player in myocardial mechanics, signaling, and disease. *Circ Res* 94:284–295
24. Duan F, Xie M, Wang X, Li Y, He L, Jiang L, Fu Q (2012) Preliminary clinical study of left ventricular myocardial strain in patients with non-ischemic dilated cardiomyopathy by three-dimensional speckle tracking imaging. *Cardiovasc Ultrasound* 10:8
25. Notomi Y, Popovic ZB, Yamada H, Wallick DW, Martin MG, Orszak SJ, Shiota T, Greenberg NL, Thomas JD (2008) Ventricular untwisting: a temporal link between left ventricular relaxation and suction. *Am J Physiol Heart Circ Physiol* 294:H505–H513